Effects of Recline on Passenger Posture and Belt Fit

Matthew P. Reed
Sheila M. Ebert

University of Michigan Transportation Research Institute

Final Report

UMTRI-2018-2

September 2018

Technical Report Documentation Page

1. Report No.	2. Government Accession No.	3. Recipient's Catalog No.
UMTRI-2018-2		

Effects of Recline on Passenger Posture and Belt Fit	5. Report Date
	6. Performing Organization Code
7. Author(s) Reed, M.P. and Ebert, S.M	8. Performing Organization Report No.
9. Performing Organization Name and Address University of Michigan Transportation Research Institute 2901 Baxter Road Ann Arbor MI 48109	10. Work Unit No. (TRAIS)
	11. Contract or Grant No.
12. Sponsoring Agency Name and Address Humanetics Innovative Solutions	13. Type of Report and Period Covered
	14. Sponsoring Agency Code
15. Supplementary Notes	

16. Abstract

Highly reclined postures may be common among passengers in future automated vehicles. Detailed data on posture and seat belt fit in such postures is needed to design appropriate seats and restraints but is not currently available. A laboratory study was conducted in which 24 men and women with a wide range of body size were measured in a typical front vehicle seat at seat back angles of 23, 33, 43, and 53 degrees. Data were gathered with and without a sitter-adjusted headrest. Posture was characterized by the locations of skeletal joint centers estimated from digitized surface landmarks. Regression analysis demonstrated that lumbar spine flexion decreased with increasing recline, and the differences between supported and unsupported head and neck postures were greater at larger recline angles. The lap portion of the three-point belt was more rearward relative to the pelvis in more-reclined postures, and the torso portion crossed the clavicle closer to the midline of the body. The regression models developed in this study will be useful for the design and assessment of seats and restraints for future vehicles.

17. Key Words	18. Distribution Statement
Vehicle occupant posture, seat belt fit	

19. Security Classif. (of this report)	20. Security Classif. (of this page)	21. No. of Pages	22. Price
		32	

Form DOT F 1700.7 (8-72) Reproduction of completed page authorized

Metric Conversion Chart

APPROXIMATE CONVERSIONS TO SI UNITS

SYMBOL	WHEN YOU KNOW	MULTIPLY BY	TO FIND	SYMBOL
LENGTH				
In	inches	25.4	millimeters	mm
Ft	feet	0.305	meters	m
Yd	yards	0.914	meters	m
Mi	miles	1.61	kilometers	km
AREA				
in^2	squareinches	645.2	square millimeters	mm^2
ft^2	squarefeet	0.093	square meters	m^2
yd^2	square yard	0.836	square meters	m^2
Ac	acres	0.405	hectares	ha
mi^2	square miles	2.59	square kilometers	km^2
VOLUME				
fl oz	fluid ounces	29.57	milliliters	mL
gal	gallons	3.785	liters	L
ft^3	cubic feet	0.028	cubic meters	m^3
yd^3	cubic yards	0.765	cubic meters	m^3
NOTE: volumes greater than 1000 L shall be shown in m^3				
MASS				
oz	ounces	28.35	grams	g
lb	pounds	0.454	kilograms	kg
T	short tons (2000 lb)	0.907	megagrams (or "metric ton")	Mg (or "t")
TEMPERATURE (exact degrees)				
°F	Fahrenheit	5 (F-32)/9 or (F-32)/1.8	Celsius	°C
FORCE and PRESSURE or STRESS				
lbf	poundforce	4.45	newtons	N
lbf/in^2	poundforce per square inch	6.89	kilopascals	kPa

LENGTH				
mm	millimeters	0.039	inches	in
m	meters	3.28	feet	ft
m	meters	1.09	yards	yd
km	kilometers	0.621	miles	mi
AREA				
mm^2	square millimeters	0.0016	square inches	in^2
m^2	square meters	10.764	square feet	ft^2
m^2	square meters	1.195	square yards	yd^2
ha	hectares	2.47	acres	ac
km^2	square kilometers	0.386	square miles	mi^2
VOLUME				
mL	milliliters	0.034	fluid ounces	fl oz
L	liters	0.264	gallons	gal
m^3	cubic meters	35.314	cubic feet	ft^3
m^3	cubic meters	1.307	cubic yards	yd^3
MASS				
g	grams	0.035	ounces	oz
kg	kilograms	2.202	pounds	lb
Mg (or "t")	megagrams (or "metric ton")	1.103	short tons (2000 lb)	T
TEMPERATURE (exact degrees)				
ºC	Celsius	1.8C+32	Fahrenheit	ºF
FORCE and PRESSURE or STRESS				
N	Newtons	0.225	poundforce	lbf
kPa	Kilopascals	0.145	poundforce per square inch	lbf/in^2

*SI is the symbol for the International System of Units. Appropriate rounding should be made to comply with Section 4 of ASTM E380.
(Revised March 2003)

ACKNOWLEDGMENTS

This research was supported by Humanetics Innovative Solutions. We thank Laura Malik for her conscientious data collection.

CONTENTS

ABSTRACT

Highly reclined postures may be common among passengers in future automated vehicles. Detailed data on posture and seat belt fit in such postures is needed to design appropriate seats and restraints but is not currently available. A laboratory study was conducted in which 24 men and women with a wide range of body size were measured in a typical front vehicle seat at seat back angles of 23, 33, 43, and 53 degrees. Data were gathered with and without a sitter-adjusted headrest. Posture was characterized by the locations of skeletal joint centers estimated from digitized surface landmarks. Regression analysis demonstrated that lumbar spine flexion decreased with increasing recline, and the differences between supported and unsupported head and neck postures were greater at larger recline angles. The lap portion of the three-point belt was more rearward relative to the pelvis in more-reclined postures, and the torso portion crossed the clavicle closer to the midline of the body. The regression models developed in this study will be useful for the design and assessment of seats and restraints for future vehicles.

INTRODUCTION

Increasing road vehicle automation is expected to lead to changes in passenger activities. Among the most common predictions is that reclined postures associated with rest will become more prevalen. Currently, little is known about the details of reclined passenger postures, including typical body segment angles. Data-based posture-prediction models have been developed for passengers (Park et al. 2016b), but these are limited to seat back angles (SAE A40) of 30 degrees. Crash safety is a prominent concern with reclined postures. Recent simulation studies have suggested that protecting passengers in highly reclined postures is challenging due to differences in occupant kinematics (Lin et al. 2018), but the postures used in those studies were not based on actual passenger data.

To address this gap, the current study examined the postures of a diverse group of passengers across a range of seat back angles. Data were gathered with and without head support at seat back angles up to 53 degrees. Lap and shoulder belt fit relative to the pelvis and clavicle were also quantified.

METHODS

Twenty-four adults (12 men and 12 women) participated in this study. The mean stature of the group was 1694 mm with a range of 1521 to 1898 mm, mean BMI was 28.9 kg/m^2 with a range of 21.0 to 37.2 kg/m^2, and mean age was 47 years with a range of 18 to 71 years. Figures 1 and 2 and Tables 1-3 show the size distribution of the participants. Standard anthropometric dimensions, including stature, body weight, and linear breadths and depths were gathered from each participant to characterize the overall body size and shape. All testing including standard anthropometric dimensions was conducted with the participants in clad in light cotton pants and shirt.

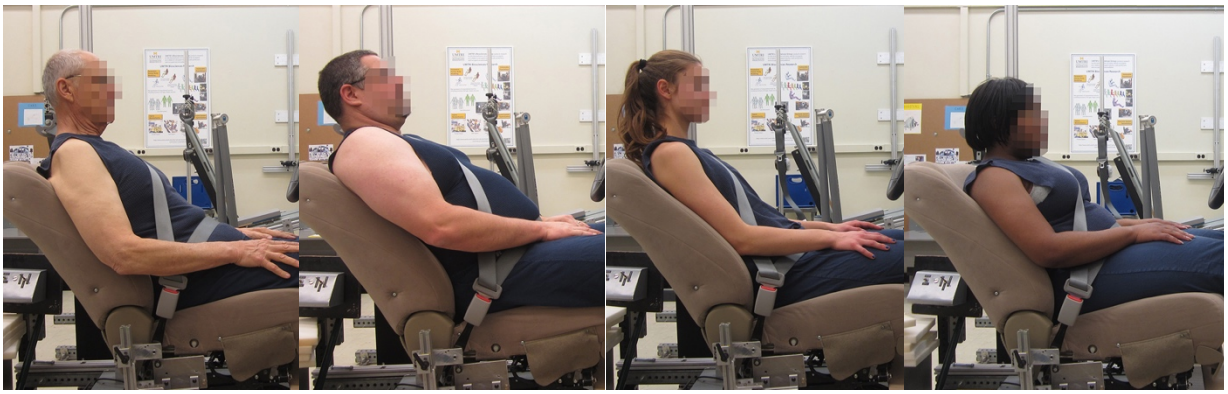

Figure 1. Study participants with a range of stature and BMI.

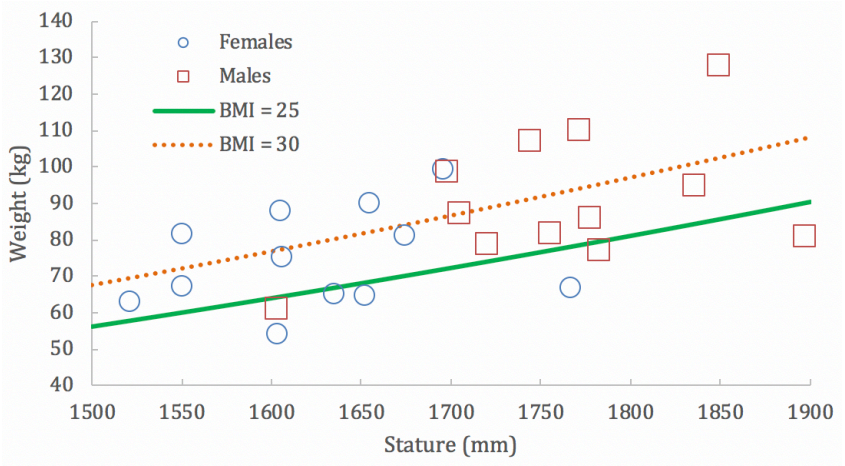

Figure 2. Participant body weight and stature.

Table 1
Participant Anthropometric Dimensions: Men and Women

Dimension	Mean	SD	Minimum	Maximum
Age (yr)	48	18	18	71
Stature with shoes (mm)	1722	109	1548	1967
Stature without shoes (mm)	1694	100	1521	1898
Weight without shoes (kg)	82.6	17.5	54.1	127.4
BMI (kg/m^2)	28.7	4.9	21.0	37.2
Erect Sitting Height (mm)	883	57	782	983
Eye Height Sitting (mm)	772	55	677	874
Acromial Height Sitting (mm)	588	44	515	661
Knee Height (mm)	518	38	459	607
Head Length (mm)	196	10	176	219
Tragion to Top of Head (mm)	126	8	114	144
Head Breadth (mm)	155	6	142	168
Shoulder-Elbow Length (mm)	370	25	332	419
Elbow-Hand Length (mm)	463	32	404	520
Maximum Hip Breadth (mm)	397	32	341	448
Buttock-Knee Length (mm)	608	39	546	682
Buttock-Popliteal Length (mm)	503	31	450	555
Bi-Acromial Breadth (mm)	386	29	338	443
Shoulder Breadth (mm)	458	35	394	532
Bi-ASIS Breadth (mm)	234	19	195	272

Table 2
Participant Anthropometric Dimensions: Women Only

Dimension	Mean	SD	Minimum	Maximum
Age (yr)	51	18	21	71
Stature with shoes (mm)	1650	73	1548	1793
Stature without shoes (mm)	1626	69	1521	1767
Weight without shoes (kg)	74.6	13.4	54.1	99.2
BMI (kg/m^2)	28.2	4.9	21.0	34.5
Erect Sitting Height (mm)	846	45	782	944
Eye Height Sitting (mm)	736	42	677	814
Acromial Height Sitting (mm)	558	32	515	621
Knee Height (mm)	496	25	459	524
Head Length (mm)	188	7	176	200
Tragion to Top of Head (mm)	121	6	114	130
Head Breadth (mm)	152	6	142	163
Shoulder-Elbow Length (mm)	355	16	332	379
Elbow-Hand Length (mm)	439	20	404	462
Maximum Hip Breadth (mm)	400	34	343	448
Buttock-Knee Length (mm)	589	28	546	631
Buttock-Popliteal Length (mm)	492	29	450	532
Bi-Acromial Breadth (mm)	363	16	338	384
Shoulder Breadth (mm)	436	28	394	495
Bi-ASIS Breadth (mm)	232	21	195	272

Table 3
Participant Anthropometric Dimensions: Men Only

Dimension	Mean	SD	Minimum	Maximum
Age (yr)	44	19	18	70
Stature with shoes (mm)	1795	92	1629	1967
Stature without shoes (mm)	1762	78	1603	1898
Weight without shoes (kg)	90.7	17.9	60.7	127.4
BMI (kg/m^2)	29.1	5.1	22.4	37.2
Erect Sitting Height (mm)	920	42	839	983
Eye Height Sitting (mm)	807	43	719	874
Acromial Height Sitting (mm)	617	33	565	661
Knee Height (mm)	541	35	470	607
Head Length (mm)	203	7	191	219
Tragion to Top of Head (mm)	131	7	120	144
Head Breadth (mm)	158	4	150	168
Shoulder-Elbow Length (mm)	385	23	349	419
Elbow-Hand Length (mm)	486	24	459	520
Maximum Hip Breadth (mm)	394	32	341	445
Buttock-Knee Length (mm)	628	39	571	682
Buttock-Popliteal Length (mm)	514	30	460	555
Bi-Acromial Breadth (mm)	408	21	371	443
Shoulder Breadth (mm)	480	27	435	532
Bi-ASIS Breadth (mm)	236	18	213	268

Vehicle Mockup

A vehicle mockup used in previous studies of driver posture was modified for use in the current testing. The mockup (Figure 3) was equipped with a six-way power seat from a 2010 Toyota Highlander with a power recline adjuster. The seat pan angle was locked at 14.5 degrees (SAE J826) and the seat moved rearward to a position where the participant's feet could not contract the pedals. The H-point of the seat was set to 270 mm above the mockup floor. The original head restraint was removed from the seat. A "head rest base" was built from a padded board attached to metal rods that inserted into the head restraint receptacles in the seat back (Figure 4). The base was easily removed, and its front surface was set back from the seat back surface farther than a normal vehicle head restraint to provide flexibility during testing. Note that this support is termed a "head rest" rather than "head restraint" because it was not designed to be appropriate for rear-impact protection or to comply with head restraint requirements. Instead, the goal was to determine appropriate geometry for comfortable head/neck support for passengers.

Figure 3. Test seat with power recline.

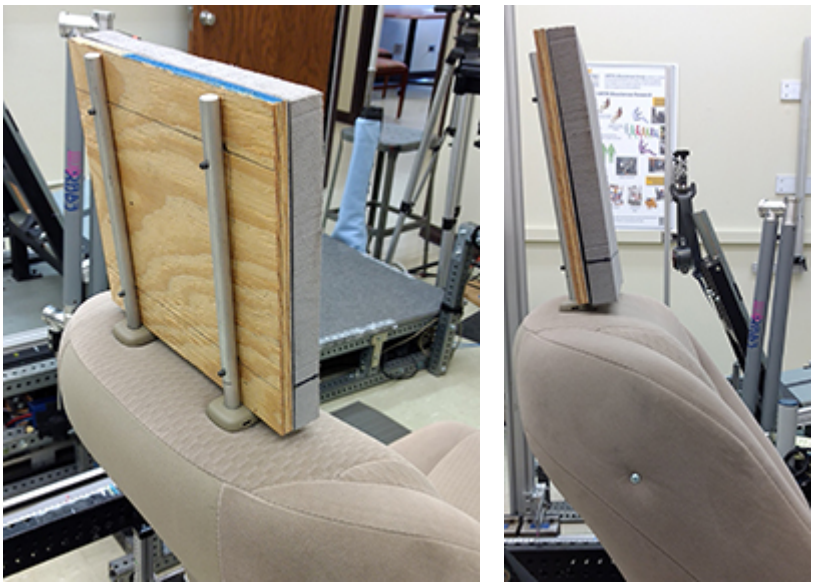

Figure 4. Removable head rest base. Additional padding was applied to obtain comfortable supported head positions – see text.

A seat belt assembly with a sliding latchplate and retractor from the second row of a model year 2010 Toyota Sienna was mounted on customized fixtures designed to permit adjustment of belt anchorage locations. A second-row belt was used to ensure sufficient webbing length for all package conditions. A rigid buckle stalk was attached to the seat with an adjustable fixture. The outboard lower anchorage was attached to the mockup, rather than to the seat, simulating a belt mounted to the vehicle body. The retractor and D-ring were mounted to a fixture allowing the D-ring location to be adjusted over a wide range. The belt webbing width was 45 mm.

Test Conditions

The seat back angle (SAE A40, also known as manikin torso angle) was initially set to 23 degrees as measured with the SAE J826 H-point machine and procedures. The seat back was rotated relative to this measurement position to achieve a range of recline angles. The pivot point of the seat back was 164 mm rearward and 86 mm down from seat H-point. The seat back was rotated 10, 20 and 30 degrees rearward to achieve nominal seat back angles of 33, 43, and 53 degrees. Note that SAE A40 was only measured at 23 degrees.

The pivot point of the upper belt anchorage (D-ring bolt) was located 312 mm rearward, 235 mm outboard and 626 mm up from the seat H-point of the 23-degree back angle condition. The upper anchorage location was rotated around the seat pivot point to keep it at the same location relative to the seat back for each of the more reclined seat back conditions. The seat pan and the lower belt anchorages were in fixed positions. The lower anchorages were mounted at an angle of 52 degrees up from horizontal with respect to the H-point in the 23-degree seat back angle condition. Figure 5 illustrates the seat back angles and upper anchorage locations.

Table 4 lists the eight test conditions that were presented to the subjects in random order. A head rest was provided in half of the conditions. In the conditions with the head rest the participant adjusted the head rest position by adding padding in front of the head rest base to obtain

comfortable head support. In the conditions without the head rest the base was removed from the seat.

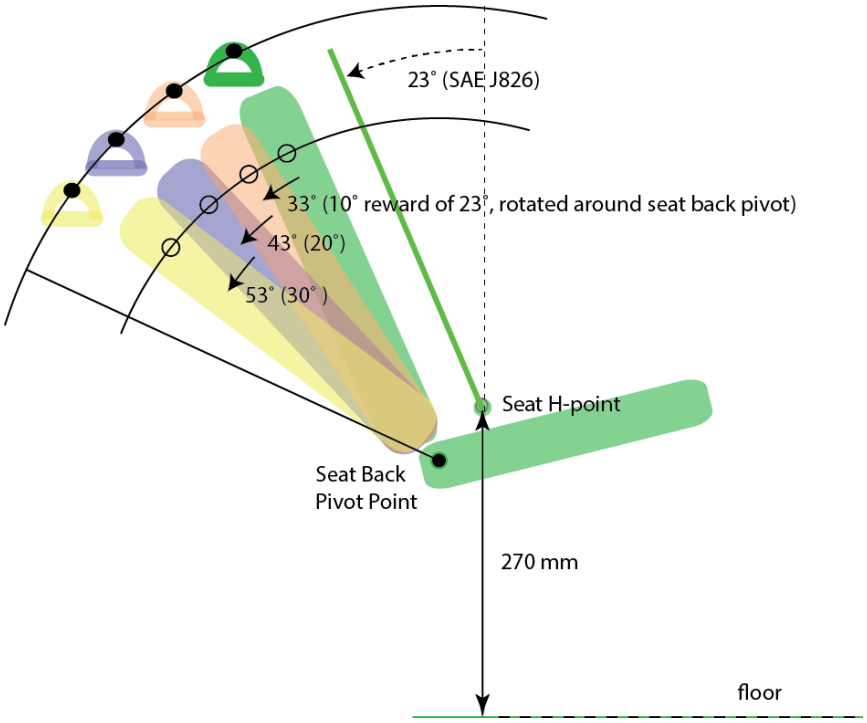

Figure 5. Illustration of test conditions.

Table 4
Test Matrix

Cond. Name	Back Angle (deg) *	Head Rest	D-ring Location Re H-point from BA 23° (mm)			D-ring Angle Re H-point from BA 23° (deg.)		D-ring Location Re Seat Pivot (mm)		D-ring Angle Re Pivot (deg.)	Outboard Lower Anchor Location re H-point from BA 23° (mm)			Outboard Lower Anchor Location re H-point from BA 23° (mm)		
			X	Y	Z	XZ	YZ	X	Z	XZ	X	Y	Z	X	Y	Z
HY23	23	Yes	312	-235	626	27	21	148	712	11.75	160	-330	-212	97	270	-127
HN23	23	No	312	-235	626	27	21	148	712	11.75	160	-330	-212	97	270	-127
HY33	33	Yes	433	-235	589	37	21	269	675	21.75	160	-330	-212	97	270	-127
HN33	33	No	433	-235	589	37	21	269	675	21.75	160	-330	-212	97	270	-127
HY43	43	Yes	547	-235	532	46	21	383	618	31.75	160	-330	-212	97	270	-127
HN43	43	No	547	-235	532	46	21	383	618	31.75	160	-330	-212	97	270	-127
HY53	53	Yes	648	-235	456	55	21	484	542	41.75	160	-330	-212	97	270	-127
HN53	53	No	648	-235	456	55	21	484	542	41.75	160	-330	-212	97	270	-127

* Seat back angle set to 23° with J826 H-point machine. More-reclined angles set by rotating seat back around seat back pivot point in increments of 10 degrees.

23˚ angle No head rest		
33˚ angle No head rest		
43˚ angle No head rest		
53˚angle No head rest		

Figure 6. Example of participants in test conditions without head rest

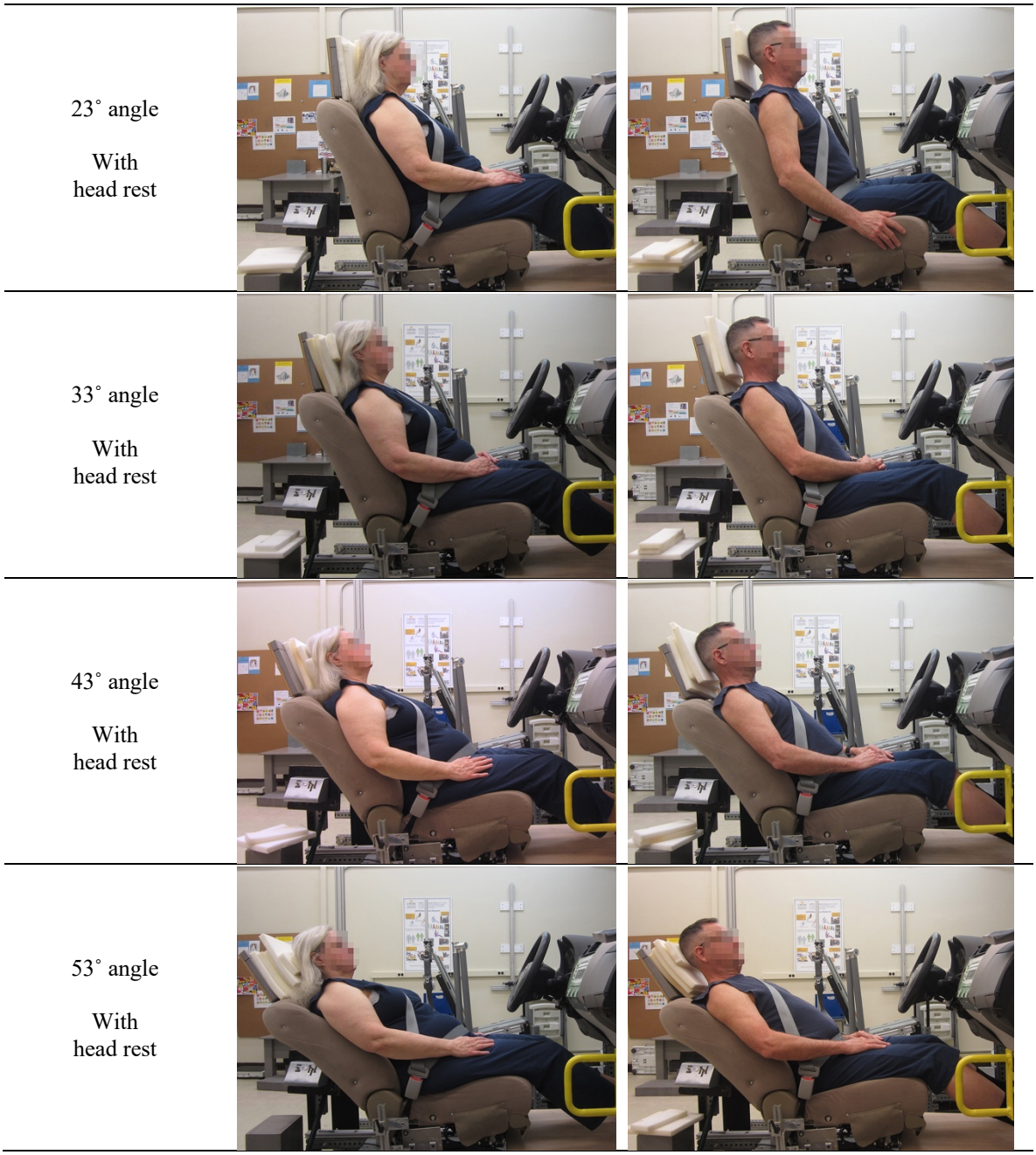

Figure 7. Example of participants in test conditions with participant-selected head rest location

Testing Protocol

The study protocol was approved by an institutional review board for human-subject research at the University of Michigan (HUM00142287). After giving written informed consent, the participants changed into the testing clothes, underwent standard anthropometry, and then had their posture measured in the test vehicle as well as a laboratory hard seat.

Testing Sequence and Data Collection

For each condition, the investigator adjusted the seat back angle to 23 degrees and asked the participant to be seated and to make themselves comfortable. The investigator then reclined the seat back to the test condition angle. The participant readjusted their posture if necessary for comfort and donned the seatbelt. If the condition did not include the head rest, the participants were asked to hold their head in a position that allowed them to look straight forward to the horizon. If the head rest was included, the participant was given a selection of foam sections of 23 mm thickness to place behind their heads until they achieved a posture that would be comfortable for "a long rest with eyes closed". Table 5 lists script text and Figure 8 shows how the participant placed the foam.

Table 5
Scripted Instructions Read Aloud by Investigator

1) Please have a seat and get comfortable

(investigator reclines seatback to condition angle)

2) Now that the seatback is adjusted, please put on the seatbelt and make sure you are still comfortable in the seat

3) Head position
    a. [If head rest is present]: Please place these foam blocks behind your head until your head and shoulders are in a position that is comfortable for a long rest with your eyes closed.
    b. [If head rest is **not** present]: Please hold your head so that you can look straight ahead toward the horizon.

4) Please place your hands on your thighs and your legs out with your feet on your heels

5) Please adjust your body again until you are comfortable – as though you were going to go for a long ride

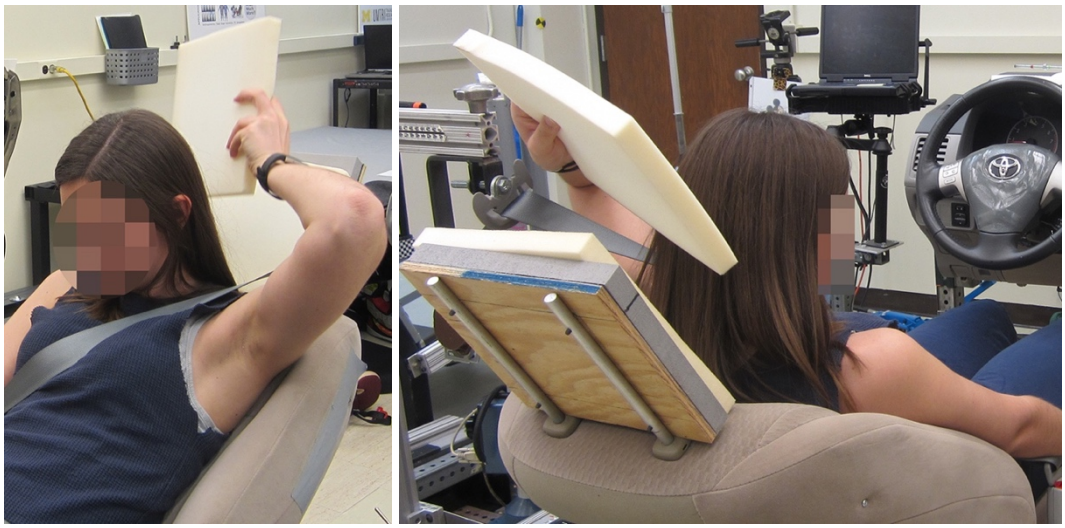

Figure 8. Participant placing foam sections behind her head to achieve comfortable support.

The investigator used the FARO Arm coordinate digitizer to record the three-dimensional locations of landmarks on the participant's body and on the mockup, seat, and belt (Table 6). In addition, a stream of points with approximately 5-mm spacing was recorded along the edges of lap and shoulder portions of the belt between the anchorages and latch plate (Figure 9).

Due to the difficulty of locating the ASIS points on obese participants, the investigator used the tool in Figure 10 to assist in digitizing the ASIS points in the vehicle mockup. The distance between the ASIS points (bispinous breadth) measured with a caliper anthropometer away from the mockup where the investigator had better access to the lap area. With the breadth marked on the tool, the tool was centered on the lap of the participant. The investigator then began palpating the abdomen at these locations and firmly compressed the flesh over the ASIS while digitizing.

Table 6
Points and streams digitized in the vehicle mockup

Participant	Mockup Seat
C7 (Cervicale)	Seat pan reference points
Back of head (max rearward)	Seat back reference point
Top of head (max height)	
Tragion, Lt	Restraint System
Ectoorbitale, Lt	D-ring reference point
Infraorbitale at pupil center , Lt	Lower anchorage reference points
Glabella	
Suprasternale	Shoulder Belt
Substernale	Inboard and outboard edge on clavicle
Medial clavicle, Lt	Top and bottom edge at participant's midline
Lateral clavicle, Lt	Inboard edge at participant's Suprasternale height
Anterior of acromion,L	
Lateral humeral epicondyle, Lt	
Lateral ulnar styloid process, Lt	
ASIS, Lt and Rt	Lap Belt
Suprapatella,Lt and Rt	Top edge and bottom edge at ASIS lateral position (Lt and Rt) and at participant's midline
Infrapatellat ,Lt and Rt	
Lateral femoral epicondyle Rt	
Medial femoral epicondyle Lt	
Toe (bottom edge of sole, longest shoe point), Lt and Rt	Seat Belt Streams
Lateral ball of foot, Lt	Top/ inboard edge of the shoulder belt from latch plate to D-ring
Heel (bottom edge of sole at midline), Lt and Rt	Top edge of the lap belt from latch plate to as close to the lower outboard anchor as possible
Lateral malleolus, Lt	
Medial ball of foot, Rt	
Medial malleolus, Rt	
Streams of points	
Sagittal line running anteriorly from shoulder to knee	
Cross body at umbilicus height	
Along superior margin of neck/shoulder area	

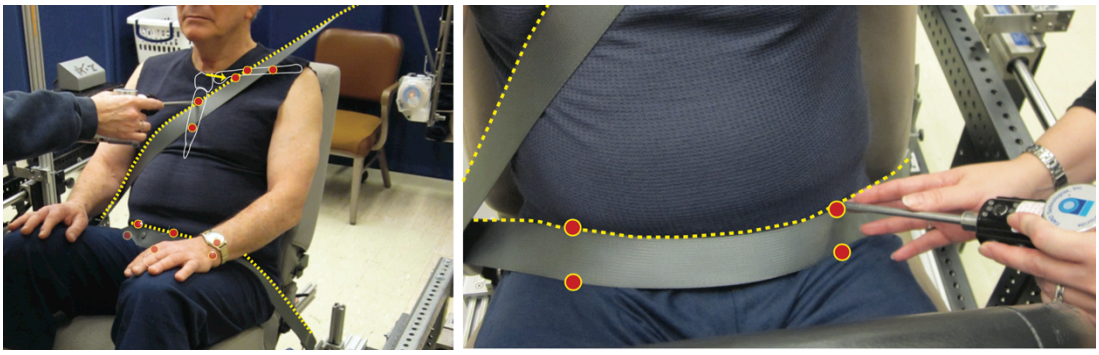

Figure 9. Continuous streams of point data (dashed line) were collected along the entire length of the webbing in addition to point data (red circles). Both the shoulder and lap belt were recorded along the upper edge of the webbing.

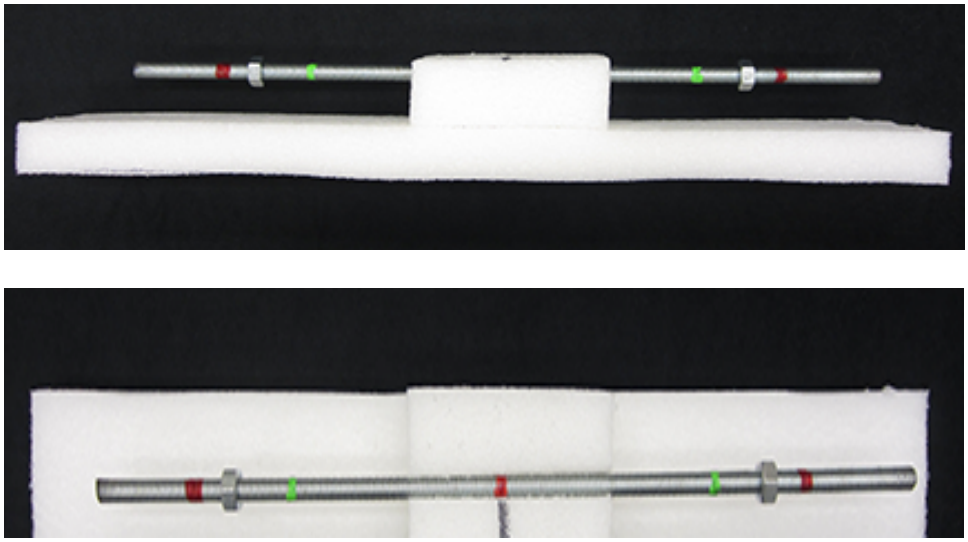

Figure 10. Tool used to aid in finding the ASIS points in the vehicle mockup. The locations of the nuts on the threaded rod were adjusted to the participants bispinous (bi-ASIS) breadth recorded during standard anthropometry

Hardseat Measurement

Body landmark locations were recorded in the laboratory hardseat shown in Figure 11. The hardseat allows access to posterior spine and pelvis landmarks that are inaccessible in the automotive seat. Figure 12 references the adjustment for adiposity described in Reed et al. (2013) was applied to the points recorded on the pelvis. The hardseat has a 14.5-degree "cushion" (pan) angle and a 23-degree back angle designed to produce postures similar to those in an automotive seat. Table 7 lists the landmarks recorded in the hardseat.

Figure 11. Hardseat with back opening (left) that allows access to posterior spine and pelvis as shown in center photo.

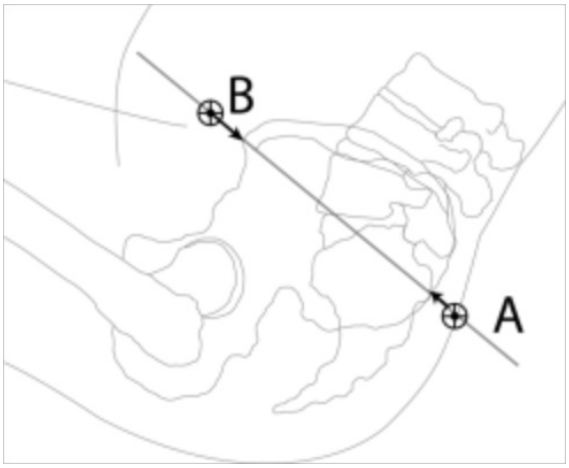

Figure 12. Compensation for adiposity at the PSIS flesh margin (A) and ASIS flesh margin (B) separating the depressed surface landmark from the underlying bone landmark (Reed et al. 2013).

Table 7
Landmarks digitized in hardseat

Back of head	Lateral femoral epicondyle, Lt and Rt	C7
Top of head (vertex)	Medial femoral epicondyle, Lt and Rt	T4
Tragion, Rt and Rt	Suprapatella, Lt and Rt	T8
Ectoorbitale, Lt and Rt	Infrapatella, Lt and Rt	T12
Infraorbitale at pupil center, Lt and Rt	Heel, Rt	L1
Glabella	Lateral malleolus, Rt	L2
Anterior acromion, Lt and Rt	Medial malleolus, Rt	L3
Lateral humeral epicondyle, Lateral, Rt	Lateral ball of foot, Rt	L4
Ulnar styloid process, Rt	Medial ball of foot, Lt	L5
Suprasternale	Toe (longest tibiale), Lt and Rt	ASIS, Lt and Rt
Substernale		PSIS, Lt and Rt

Calculating Pelvis Position and Orientation

The position and orientation of the bony pelvis is difficult to measure but of considerable importance. The methods used in the current study are based on those reported by Park et al. (2015). In brief, the steps are:

1. Using the hardseat ASIS and PSIS locations, estimate the subject-specifc pelvis geometry using an estimate flesh margin at the ASIS that is based on the adjustment for BMI presented by Reed et al. (2013). The pelvis geometry is defined by surface ASIS, surface PSIS, bone ASIS estimate, bone PSIS estimate, and estimated L5/S1 and left and right hip joint centers). Also record a "thigh length" as the distance between the suprapatellar landmark and estimated hip joint center location on each side. Also record the lumbar link length (distance from estimated T12/L1 to estimated L5/S1 joint centers).
2. In the vehicle seat data, align the subject-specific pelvis geometry to the measured mid-ASIS point and align the lateral (inter-ASIS) axis.
3. Rotate around the lateral axis such that the lumbar link length matches the hardseat value.
4. With this as a starting point, apply the optimization method described in Park et al. (2015), which finds the pelvis position and rotation around the lateral axis that best matches both the lumbar and left thigh segment lengths. The constraints were adjusted from those used by Park et al. to account for the reclined postures. Lumbar link length was permitted to deviate from the hardseat value by up to 20 mm and the pelvis angle could change up to 10 degrees forward or 45 degrees rearward from the initial value. X and Z translation constraints were 25 mm forward/45 mm rearward and 25 mm upward/50 mm downward. In all but four cases, the left thigh segment length from the hardseat was matched within 1 mm; in the remaining cases, the resulting thigh segment length was within 10 mm of the hardseat value.

Calculating Posture Variables

Landmark data from the hardseat and vehicle seat were used to characterize participant posture. Figure 13 illustrates the primary variables, which are based on the models

reported by Reed et al. (2002) and Park et al. (2016a, 2016b). The mean hip location (average of left and right hip joint centers) was computed with respect to the seat H-point location. The side-view orientations of the pelvis, lumbar, thorax, and neck segments were computed with respect to vertical (positive values indicate reclined from vertical). Head orientation was defined as the angle of the Frankfurt plane with respect to forward horizontal (positive with eyes up). The thigh angle was computed in side view with respect to forward horizontal, and the leg angle was reported positive rearward of vertical. Overall torso recline was quantified by the angle of the side-view vector from mean hip to eye (estimate of the center of the left eyeball) with respect to vertical.

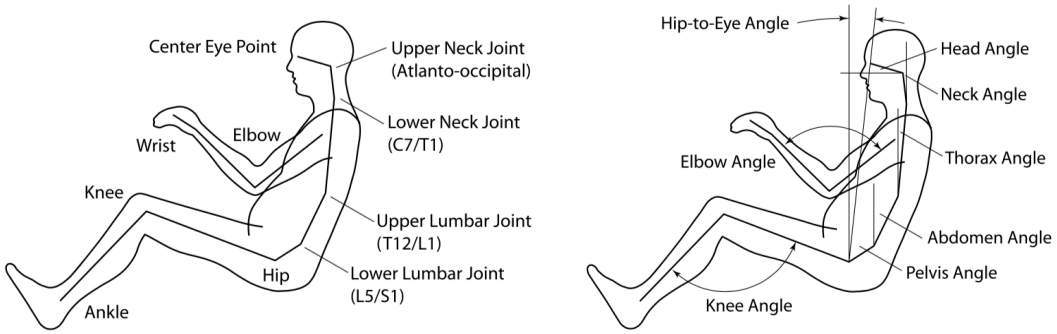

Figure 13. Posture variables.

Calculating Belt Fit

Following methods used in a previous belt fit studies (Reed et al. 2012, Reed et al. 2013), lap belt fit was quantified by the fore-aft and vertical location of the upper/rearward margin of the lap portion of the belt at the lateral location of the anterior-superior iliac spine (ASIS) landmarks on the left and right sides of the pelvis (Figures 14 and 15). The correction for adiposity at the ASIS landmarks documented in Reed et al. (2013) was used. Shoulder belt fit was quantified by the lateral location of the inboard edge of the shoulder portion of the belt relative to the body midline at the height of the suprasternale landmarks (Figure 16). The Y-axis (medial lateral) distance between the body midline and belt is termed shoulder belt score (Reed et al. 2013). A fifth-order Bézier curve was fit to the lap and shoulder belt stream points to smooth measurement error. The amount of belt feed out was calculated by finding the lengths of the lap belt between the lower outboard anchor and the buckle and the shoulder belt between the D-ring and buckle calculated along the Bézier curve.

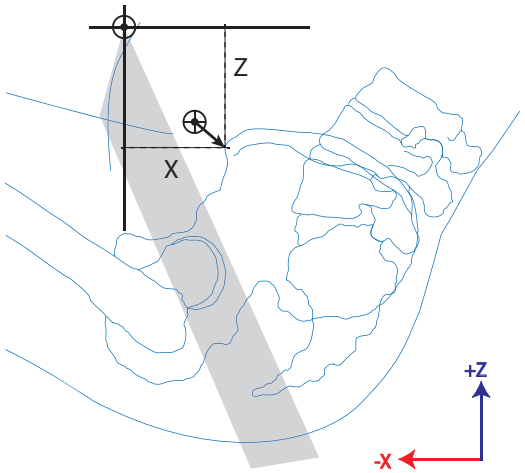

Figure 14. Locations of points recorded on the lap belt

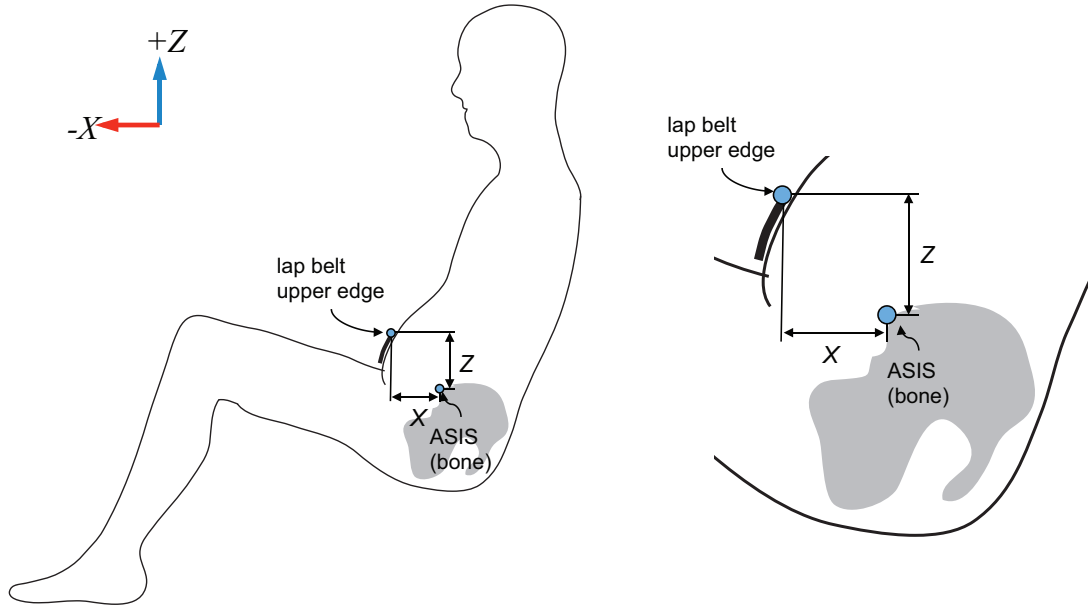

Figure 15. Dependent measures for lap belt fit. The upper/rearward edge of the lap portion of the belt is measured at the lateral position of the right and left the predicted ASIS location. The fore-aft (X) coordinate is positive rearward of the ASIS and the vertical coordinate is positive above the ASIS landmark.

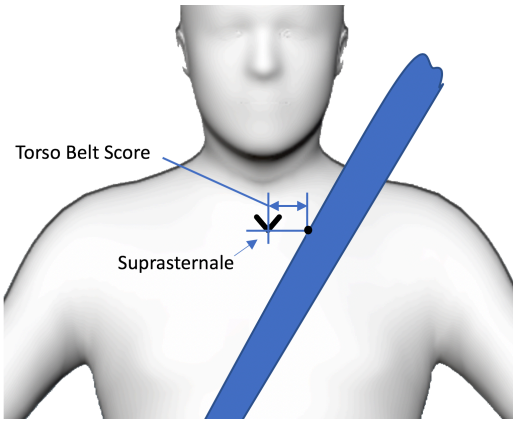

Figure 16. Torso (shoulder) belt fit measurement. Larger positive values indicate more-outboard belt placement.

Statistical Analysis

The effects of test conditions and participant characteristics were examined using a range of plotting methods as well as linear regression and ANOVA. Potential two-way interactions between participant characteristics and test conditions were considered, and trends were examined within sex as well as with the pooled male/female population. When developing posture-prediction models using regression, terms were included only if they were significant with $p<0.01$ and the addition of the term increased the adjusted R^2 value (i.e., fraction of variance accounted for by the model) by at least 0.02.

RESULTS

Posture

Hip Location

The mean hip location with respect to seat H-point was not strongly affected by either the experimental variables or participant characteristics. On average, the mean hip location was 11 mm below and 16 mm rearward of the seat H-point. The mean hip location was significantly further forward at BA53, but the difference relative to the other conditions was less than half of the standard deviation within condition. Head rest condition did not affect hip location.

Table 8
Mid-hip Location for All Participants

Back Angle (deg)	X*	X SD	Z	Z SD
23	11.3	20.9	-11.7	13.8
33	12.5	22.4	-12.9	13.2
43	14.8	22.1	-10.2	13.7
53	25.5	23.9	-8.4	14.8

* Positive values indicate the hip location is forward of seat H-point.

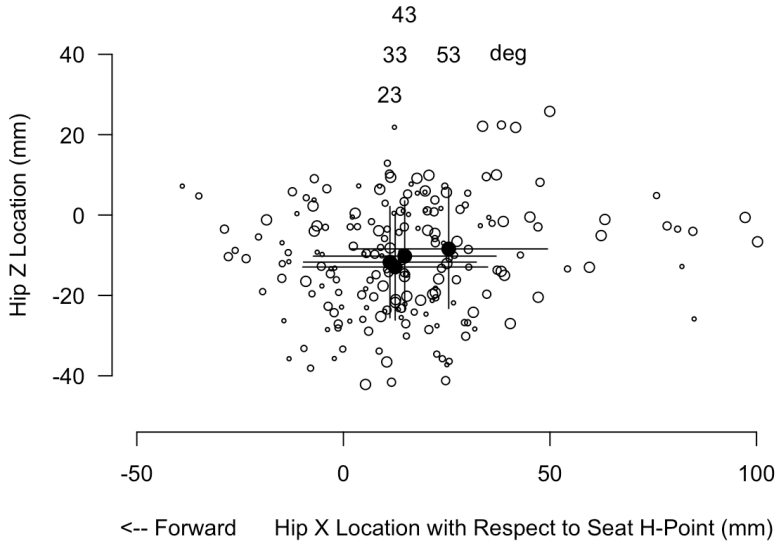

Figure 17. Hip locations for each subject and condition by back angle. Means ± 1 sd at each back angle are shown. Larger symbols indicate group means. Data from larger back angles are shown with larger symbols.

Body Segment Angles

Tables 9 and 10 list body segment angle results for the head-rest and no-head-rest conditions. These tables summarize the variable values across subjects, so the effects of body dimensions are not considered. Table 11 lists regression functions for these variables that incorporate anthropometric predictors.

Table 9
Body Segment Angles – No Head Rest

Variable (deg)	Seat Back Angle (deg)							
	23		33		43		53	
	Mean	SD	Mean	SD	Mean	SD	Mean	SD
Pelvis Angle	52.7	9.3	60.6	11.8	63.1	15.4	59.6	32.8
Lumbar Angle	20.6	8.0	30.3	8.2	41.3	12.6	48.5	11.6
Thorax Angle	6.5	4.4	15.1	4.6	24.3	5.6	33.5	6.0
Neck Angle	1.3	5.2	4.4	7.4	9.7	8.5	19.0	10.7
Head Angle	0.3	7.0	-0.2	7.0	4.7	9.8	12.2	13.3
Thigh Angle	12.8	2.2	13.3	1.9	12.7	2.3	13.0	2.2
Leg Angle	47.1	5.4	47.4	5.6	47.4	5.8	48.1	5.8
Hip-Eye Angle	7.0	2.7	14.7	3.3	22.7	3.8	31.1	3.6

Table 10
Body Segment Angles – With Head Rest

Variable (deg)	Seat Back Angle (deg)							
	23		33		43		53	
	Mean	SD	Mean	SD	Mean	SD	Mean	SD
Pelvis Angle	51.0	10.1	54.3	12.7	58.6	15.1	63.3	15.3
Lumbar Angle	21.4	8.7	31.5	9.5	43.3	11.8	54.5	15.0
Thorax Angle	10.6	8.1	19.3	6.0	28.6	5.9	38.7	6.1
Neck Angle	11.4	7.8	18.6	8.0	29.6	10.3	41.0	8.9
Head Angle	7.5	10.1	13.3	9.7	23.4	10.1	34.7	8.9
Thigh Angle	12.7	2.0	12.5	2.1	12.5	2.2	10.5	4.0
Leg Angle	47.4	5.2	47.0	6.1	46.9	5.9	43.2	20.4
Hip-Eye Angle	11.0	5.8	18.9	4.1	28.4	4.1	38.4	3.4

Table 11
Regression Equations Predicting Dependent Measures

Variable (mm, deg)	Intercept	Stature	BMI	SHS	Head Rest	Back Angle	H*B	RMSE	R^2adj
HipX	79.0	-0.047				0.448		21.9	0.09
HipZ	35.2	-0.029			5.94			13.3	0.08
Pelvis Angle	84.8		-1.37			0.331		15.4	0.19
Lumbar Angle	30.2	-0.0328	0.794			1.02		9.4	0.64
Thorax Angle	-34.1		-0.670	73.9	4.44	0.919		4.8	0.84
Neck Angle	-13.6				0.834	0.584	0.413	8.5	0.67
Head Angle	-28.0		0.584		-3.62	0.406	0.501	9.3	0.59
Thigh Angle	6.00		0.226					2.3	0.19
Leg Angle	-20.9	0.040						7.8	0.22
Hip-Eye Angle	-7.5		-0.217		5.30	0.860		3.8	0.87
Hip-Eye X	-628	0.119	-1.85	671	65.6	8.60		42.3	0.86
Hip-Eye Z	-537	0.382	1.77	1101		-4.04		23.6	0.87
Cervical Flexion	41.2	0.000288	-1.26		-1.09	0.267		8.8	0.49
Lumbar Flexion	24.3	0.033	-0.643		-6.62	-0.591		15.2	0.24

* Stature (mm), BMI (kg/m^2), SHS = erect sitting height / stature, Head Rest Present = 1, Absent = 0, Back Angle = SAE A40 (see text); H*B = BackAngle (deg) * HR Present (1|0)

Table 12
Regression Equations for Segment Lengths

Variable (mm, deg)	Intercept	Stature	BMI	SHS	Head Rest	Back Angle	H*B	RMSE	R^2adj
Hip-Eye Distance	-716	0.400		1294				28.1	0.70
Leg Length	168.2	0.523		-1240				33.8	0.76
Thigh Length	723	0.256		-1294				61.5	0.36
Neck Length	-304	0.102		480.3				12.4	0.47
Thorax Length	-848	0.305		1165				18.6	0.78
Lumbar Length	206	0.004		-88.8				16.6	0.00
Pelvis Length	84.4	0.027		-51.4				4.0	0.35
Head Length	59.8	0.0136						4.4	0.09

Belt Fit

Table 13 and Figure 18 show the mean lap belt position relative to the bone ASIS on the right side of the pelvis. On average, the lap belt was forward and above the pelvis. The belt was further rearward relative to the pelvis, on average, with increasing seat back angle, but the vertical position was not significantly affected. Table 14 lists regression models for lap belt fit. BMI was the dominant predictor, with higher BMI associated with further-forward and higher lap belt positions.

Figure 19 shows the distributions of torso belt score across seat back angles. On average, the torso portion of the three-point belt was further inward with greater recline. The belt crossed the body midline at the height of the clavicle at the largest recline angle. Table 14 shows that torso belt score was significantly affected by stature, the ratio of sitting height to stature, and seat back angle. Note that the apparent nonlinear trend with seat back angle visible in Figure 19 is not statistically significant.

Table 13
Means and Standard Deviations of Lap Belt Score (mm)

Seat Back Angle (deg)	Lap Belt X		Lap Belt Z	
	Mean	SD	Mean	SD
23	-88.9	34.9	74.6	27.8
33	-82.0	27.5	75.9	27.5
43	-70.9	26.3	73.1	24.6
53	-63.4	24.5	75.3	27.9

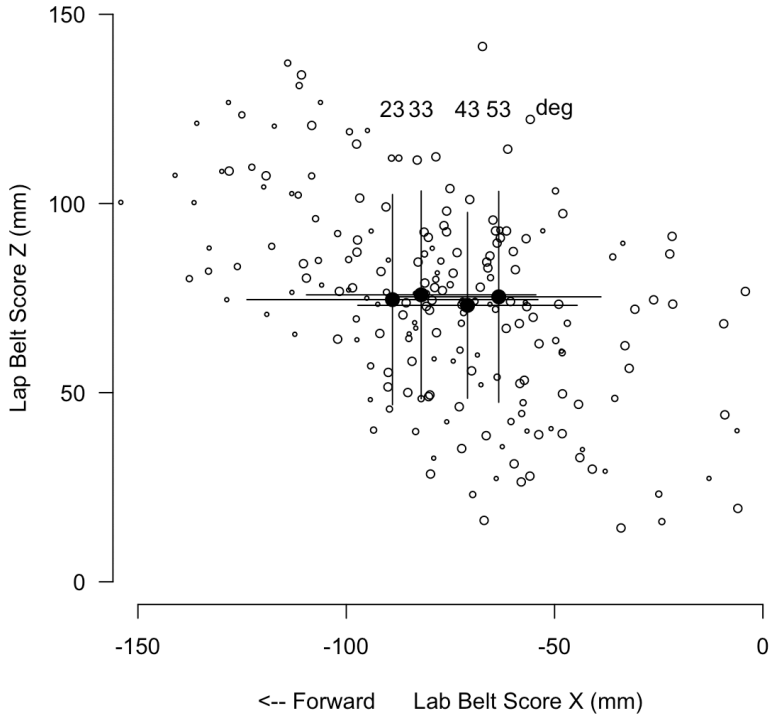

Figure 18. Distribution of lap belt locations relative to estimated bone ASIS on the right side of the pelvis. Condition means and standard deviations are shown. Data from smaller back angles are shown with smaller symbols.

Table 14
Regression Models for Lap and Torso Belt Scores

Variable (mm)	Intercept	Stature (mm)	SHS*	BMI (kg/m^2)	Seat Back Angle (deg)	(Seat Back Angle)^2 (deg)	RMSE	R^2adj
Lap Belt Score X	10.7			-4.22	0.908		19.6	0.57
Lap Belt Score Z	-139.3	0.0582		4.00			17.8	0.56
Torso Belt Score	-665	0.089	1090			-0.0258	24.3	0.55

* Erect sitting height divided by stature.

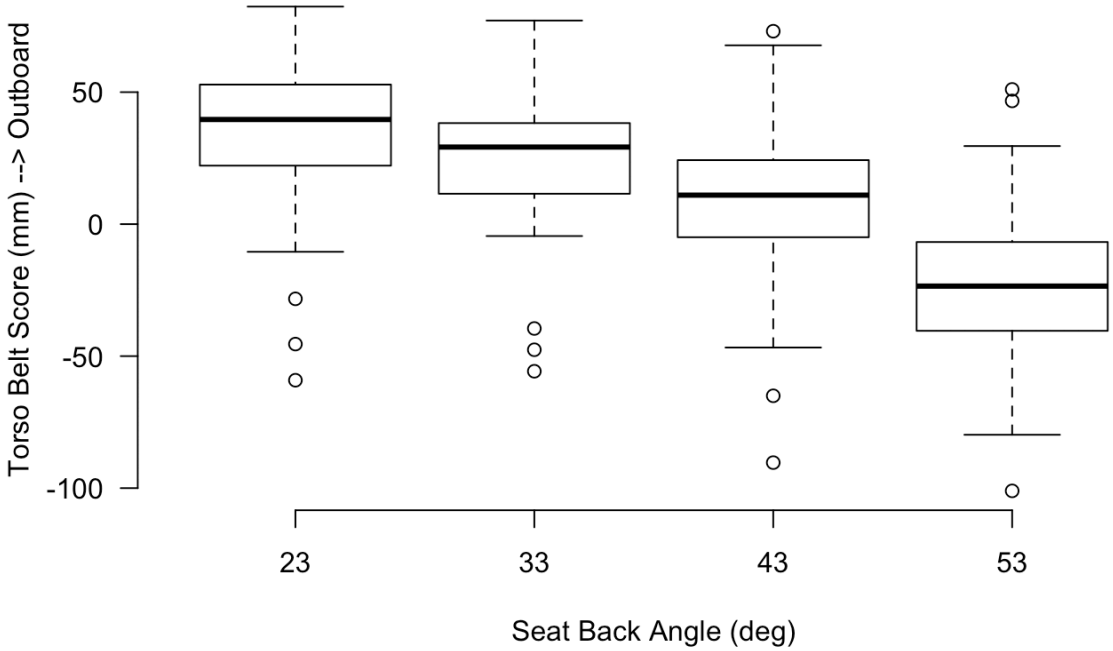

Figure 19. Torso belt score as a function of seat back angle. Higher scores are more outboard. A score of zero indicates that the inner edge of the belt lies on the body centerline at the height of the clavicle (suprasternale landmark).

DISCUSSION

This is the first detailed examination of highly reclined postures in automotive seats. Previous studies had been limited to seat back angles of 30 degrees, but the current data extend to 53 degrees and could reasonably be extrapolated to 60 degrees, based on the finding of predominantly linear effects of seat back angle on posture variables.

This study is unusual in finding hip locations slightly rearward of seat H-point, on average, even at the 23-degree seat back angle. Many previous UMTRI studies have found hip locations somewhat forward of H-point (e.g., Reed et al. 2002; Park et al. 2016). More-rearward hip locations were expected in the more-reclined conditions, because the position of the seat back angle pivot results in the seat back moving rearward behind the pelvis as it reclines. Because the order of test conditions was randomized, the finding of the hips being rearward of H-point in the 23-degree condition may be due to changes in participant behavior due to the experience of highly reclined conditions. Whether this behavior would be similar in a more realistic, on-road situation is unknown.

The pelvis rotated rearward with increasing recline but lagged behind the change in seat back angle. In contrast, the thorax moved approximately at the same rate as the seat back (coefficient 0.9), so that lumbar spine flexion decreased with increasing recline. Over the seat back angle change of 30 degrees, lumbar spine flexion decreased an average of 18 degrees. As expected, head and neck angles were affected by the use of the head rest. Significant interactions were noted with seat back angle; the difference in head/neck posture with and without the headrest was much larger at higher recline angles (see Figures 6 and 7). Interestingly, the hip location was significantly higher when using the headrest, likely due to offloading of the head weight onto the headrest.

Lap belt fit changed slightly with increased recline, with the belt shifting rearward, closer to the pelvis. However, because the vertical position with respect to the ASIS remained the same, on average, the effect of this change on lap belt performance in crash scenarios is unclear. The participants placed the shoulder belt significantly further inboard (closer to occupant centerline) at higher recline angles. Note that the participants donned the belt after finding a comfortable reclined posture. The D-ring (upper anchorage) location was rotated around the seat H-point at the same rate as the seat back, creating nominally constant belt geometry. More study is needed to understand why the belt fit changed in this way.

This study has important limitations that should be addressed in future work. A single seat was used, and this seat was not designed for highly reclined postures. Seats specifically designed for such postures may have different contours and produce different postures. The seat belt was not designed for reclined postures and only an approximation of a seat-integrated belt was presented. Posture measurements were made during a short-duration sitting session. The observed postures were largely sagittally symmetric, but long-duration, reclined postures might result in increased asymmetry. The data were also gathered in a static laboratory setting. Vehicle ride motion could result in differences in posture.

REFERENCES

Park, J., Ebert, S.M., Reed, M.P., and Hallman, J.J. (2015). Development of an optimization method for locating the pelvis in an automobile seat. *Proc. 6th International Conference on Applied Human Factors and Ergonomics*, Las Vegas, Nevada.

Park, J., Reed, M.P., and Hallman, J.J. (2016a). Statistical models for predicting automobile driving postures for men and women including effects of age. *Human Factors*, 58(2):261-278. 10.1177/0018720815610249

Park, J., Ebert, S.M., Reed, M.P., and Hallman, J.J. (2016b). A statistical model including age to predict passenger postures in the rear seats of automobiles. *Ergonomics*, 59(6):796-805, 10.1080/00140139.2015.1088076

Reed, M.P., Manary, M.A., Flannagan, C.A.C., and Schneider, L.W. (2002). A statistical method for predicting automobile driving posture. *Human Factors,* 44 (4): 557-568.

Reed, M.P., Ebert, S.M., and Hallman, J.J. (2013). Effects of driver characteristics on seat belt fit. *Stapp Car Crash Journal*, 57:43-57.

Lin, H, Gepner, B, Wu, T, Forman, J, and Panzer**,** M. (2018). Effect of Seatback Recline on Occupant Model Response in Frontal Crashes. *Proc. IRCOBI.*